CHAPTER

Control volume finite element method (CVFEM) 1

1.1 INTRODUCTION

Fluid flow has several applications in engineering and nature. Mathematically, real flows are governed by a set of nonlinear partial differential equations in complex geometry. So, suitable solutions can be obtained through numerical techniques such as the finite difference method, the finite volume method (FVM), and the finite element method (FEM). In the past decade the FEM has been developed for use in the area of computational fluid dynamics; this method has now become a powerful method to simulate complex geometry. However, the FVM is applied most in calculating fluid flows. The control volume finite element method (CVFEM) combines interesting characteristics from both the FVM and FEM. The CVFEM was presented by Baliga and Patankar [1,2] using linear triangular finite elements and by Raw and Schneider [3] using linear quadrilateral elements. Several authors have improved the CVFEM from then to now. Raw et al. [4] applied a nine-nodded element to solve heat conduction problems. Banaszek [5] compared the Galerkin and CVFEM methods in diffusion problems using six-nodded and nine-nodded elements. Campos Silva et al. [6] developed a computational program using nine-nodded finite elements based on a control volume formulation to simulate two-dimensional transient, incompressible, viscous fluid flows. Campos Silva and Moura [7] and Campos Silva [8] presented results for fluid flow problems. The CVFEM combines the flexibility of FEMs to discretize complex geometry with the conservative formulation of the FVMs, in which the variables can be easily interpreted physically in terms of fluxes, forces, and sources. Saabas and Baliga [9,10] referenced a list of several works related to FVMs and CVFEMs. Voller [11] presented the application of CVFEM for fluids and solids. Sheikholeslami et al. [12] studied the problem of natural convection between a circular enclosure and a sinusoidal cylinder. They concluded that streamlines, isotherms, and the number, size, and formation of cells inside the enclosure strongly depend on the Rayleigh number, values of amplitude, and the number of undulations of the enclosure.

1.2 DISCRETIZATION: GRID, MESH, AND CLOUD

In general there are three ways to place node points into a domain [11].

1.2.1 GRID

A basic approach assigns the location of nodes using a structured grid where, in a two-dimensional domain, the location of a node is uniquely specified by a row and a column index (Fig. 1.1a). Although such a structured approach can lead to convenient and efficient discrete equations, it lacks flexibility in accommodating complex geometries or allowing for the local concentration of nodes in solution regions of particular interest.

1.2.2 MESH

Geometric flexibility, usually at the expense of solution efficiency, can be added by using an unstructured mesh. Figure 1.1b shows an unstructured mesh of triangular elements. In two-dimensional domains triangular meshes are good selections because they can tessellate any planar surface. Note, however, that other choices of elements can be used in place of or in addition to triangular elements. The mesh can be used to determine the placement of the nodes. A common choice is to place the nodes at the vertices of the elements. In the case of triangles this allows for the

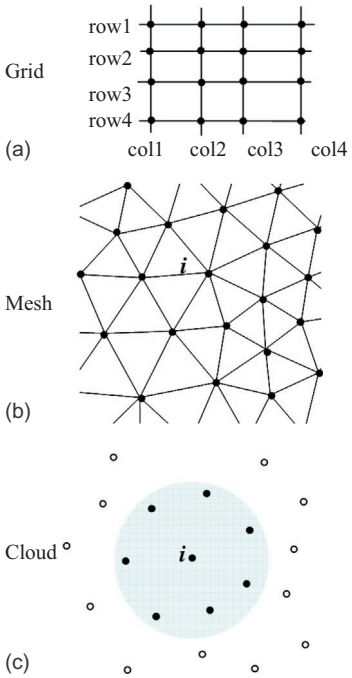

FIGURE 1.1

Different forms of discretization [11], including a grid (a), mesh (b), and cloud (c).

approximation of a dependent variable over the element, by linear interpolation between the vertex nodes. Higher-order approximations can be arrived by using more nodes (e.g., placing nodes at midpoints) or alternative elements (e.g., quadrilaterals). When considering an unstructured mesh recognizing the following is important:

1. The quality of the numerical solution obtained is critically dependent on the mesh. For example, avoiding highly acute angles is a key quality requirement for a mesh of triangular elements. The generation of appropriate meshes for a given domain is a complex topic worthy of a monograph in its own right. Fortunately, for two-dimensional problems in particular, there is a significant range of commercial and free software that can be used to generate quality meshes.
2. The term *unstructured* is used to indicate a lack of a global structure that relates the position of all the nodes in the domain. In practice, however, a local structure—the region of support—listing the nodes connected to a given node i is required. Establishing, storing, and using this local data structure is one of the critical ingredients in using an unstructured mesh.

1.2.3 CLOUD

The most flexible discretization is to simply populate the domain with node points that have no formal background grid or mesh connecting the nodes. Solution approaches based on this "meshless" form of discretization create local and structures, usually based on a "cloud" of neighboring nodes that fall within a given length scale of a given node i [13] (Fig. 1.1c).

1.3 ELEMENT AND INTERPOLATION SHAPE FUNCTIONS

A building block of discretization is the triangular element (Fig. 1.2). For linear triangular elements the node points are placed at the vertices. In Fig. 1.2, the nodes, moving in a counterclockwise direction, are labeled 1, 2, and 3. Values of the dependent variable ϕ are calculated and stored at these node points.

In this way, values at an arbitrary point (x, y) within the element can be approximated with linear interpolation

$$\phi \approx ax + by + c, \tag{1.1}$$

where the constant coefficients a, b, and c satisfy the nodal relationships

$$\phi_i = ax_i + by_i + c, \quad i = 1, 2, 3. \tag{1.2}$$

Equation (1.1) can be more conveniently written in terms of the shape function N_1, N_2, and N_3, where

$$N_i(x, y) = \begin{cases} 1 & \text{At node } i \\ 0 & \text{At all points on side opposite node } i \end{cases} \tag{1.3}$$

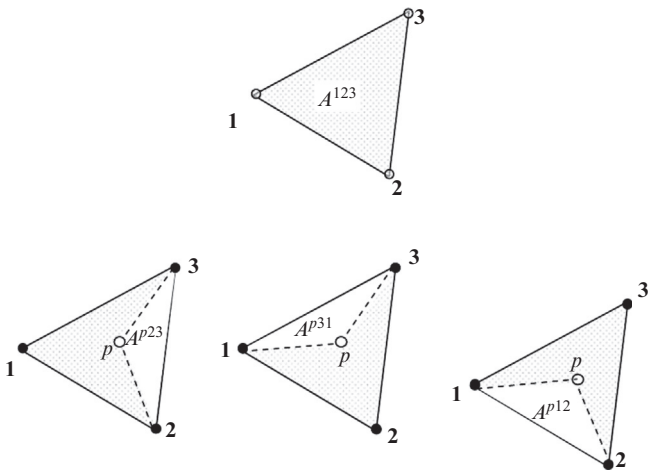

FIGURE 1.2

An element indicating the areas used in shape function definitions [11].

$$\sum_{i=1}^{3} N_i(x,y) = 1 \quad \text{At every point in the element} \tag{1.4}$$

such that, over the element the continuous unknown field can be expressed as the linear combination of the values at nodes $i = 1,2,3$:

$$\phi(x,y) \approx \sum_{i=1}^{3} N_i(x,y)\phi_i. \tag{1.5}$$

With linear triangular elements a straightforward geometric derivation for the shape functions can be obtained. With reference to Fig. 1.2, observe that the area of the element is given by

$$A^{123} = \frac{1}{2}\begin{vmatrix} 1 & x_1 & y_1 \\ 1 & x_1 & y_1 \\ 1 & x_1 & y_1 \end{vmatrix} = \frac{1}{2}[(x_2y_3 - x_3y_2) - x_1(y_3 - y_2) + y_1(x_3 - x_2)] \tag{1.6}$$

and the area of the subelements with vertices at points $(p,2,3)$, $(p,3,1)$, and $(p,1,2)$, where p is an arbitrary and variable point in the element, are given by

$$\begin{aligned} A^{p23} &= \left[(x_2y_3 - x_3y_2) - x_p(y_3 - y_2) + y_p(x_3 - x_2)\right] \\ A^{p31} &= \left[(x_3y_1 - x_1y_3) - x_p(y_1 - y_3) + y_p(x_1 - x_3)\right]. \\ A^{p12} &= \left[(x_1y_2 - x_2y_1) - x_p(y_2 - y_1) + y_p(x_2 - x_1)\right] \end{aligned} \tag{1.7}$$

Based on these definitions, it follows that the shape functions are given by

$$N_1 = A^{P23}/A^{123}, \quad N_2 = A^{P31}/A^{123}, \quad N_3 = A^{P12}/A^{123}. \tag{1.8}$$

Note that, when point p coincides with node i $(1,2,\text{or}\,3)$, the shape function $N_i = 1$, and when point p is anywhere on the element side opposite node i, the associated subelement area is zero, and, through Eq. (1.8), the shape function $N_i = 0$. Hence

the shape functions defined by Eq. (1.8) satisfy the required condition in Eq. (1.3). Further, note that at any point p, the sum of the areas:

$$A^{P23} + A^{P31} + A^{P12} = A^{123} \tag{1.9}$$

is such that the shape functions at (x_p, y_p) sum to unity. Hence the shape functions defined by Eq. (1.8) also satisfy the conditions in Eq. (1.4). For future reference, it is worthwhile to note that the following constants are the derivatives of the shape functions in Eq. (1.8) over the element:

$$\begin{aligned}
N_{1x} &= \frac{\partial N_1}{\partial x} = \frac{(y_2 - y_3)}{2A^{123}}, \quad N_{1y} = \frac{\partial N_1}{\partial y} = \frac{(x_2 - x_3)}{2A^{123}} \\
N_{2x} &= \frac{\partial N_2}{\partial x} = \frac{(y_3 - y_2)}{2A^{123}}, \quad N_{2y} = \frac{\partial N_2}{\partial y} = \frac{(x_1 - x_3)}{2A^{123}} \\
N_{3x} &= \frac{\partial N_3}{\partial x} = \frac{(y_1 - y_2)}{2A^{123}}, \quad N_{3y} = \frac{\partial N_3}{\partial x} = \frac{(x_2 - x_1)}{2A^{123}}
\end{aligned} \tag{1.10}$$

1.4 REGION OF SUPPORT AND CONTROL VOLUME

The local structure on the mesh in Fig. 1.1b is defined in terms of the region of support—the list of nodes that share a common element with a given node i [11] (Fig. 1.3). In this region of support, as illustrated in Fig. 1.3, a control volume is created by joining the center of each element in the support to the midpoints of the

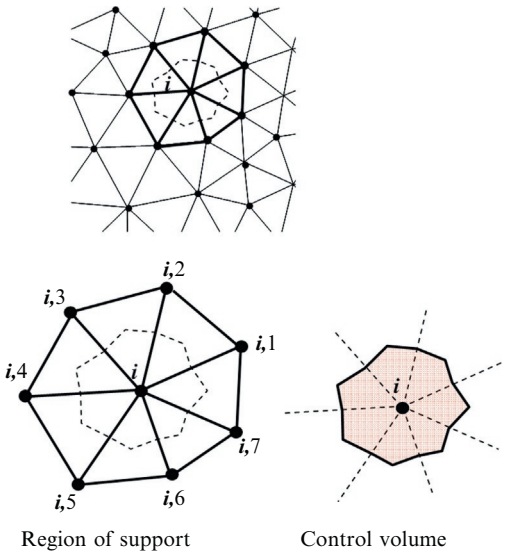

FIGURE 1.3

Region of support and control volume for node i in an unstructured mesh of linear triangular elements [11].

element sides that pass through node i. This creates a closed polygonal control volume with $2m$ sides (faces), where m is the number of elements in the support. Each element contributes one-third of its area to the control volume area, and the volumes from all the nodes tessellate the domain without overlapping.

1.5 DISCRETIZATION AND SOLUTION

1.5.1 STEADY-STATE ADVECTION-DIFFUSION WITH SOURCE TERMS

To illustrate a solution procedure using the CVFEM, one can consider the general form of advection-diffusion equation for node i in integral form:

$$-\int_V Q\,\mathrm{d}V - \int_A k\nabla\phi\cdot n\,\mathrm{d}A + \int_A (v\cdot n)\phi\,\mathrm{d}A = 0 \tag{1.11}$$

or point form

$$-\nabla\cdot(k\nabla\phi) + \nabla\cdot(v\phi) - Q = 0, \tag{1.12}$$

which can be represented by the system of CVFEM discrete equations as:

$$[a_i + Qc_i + Bc_i]\phi_i = \sum_{j=1}^{n_i} a_{i,j}\phi_{S_{i,j}} + Q_{B_i} + B_{B_i}. \tag{1.13}$$

In Eq. (1.13), the a's are the coefficients, the index (i, j) indicates the jth node in the support of node i, the index $S_{i,j}$ provides the node number of the jth node in the support, the Bs account for boundary conditions, and the Qs for source terms. For the selected triangular element shown in Fig. 1.4, this approximation (without considering the source term) leads to:

$$-\left(a_1^k + a_1^u\right)\phi_i + \left(a_2^k + a_2^u\right)\phi_{S_{i,3}} + \left(a_2^k + a_2^u\right)\phi_{S_{i,4}} = 0 \tag{1.14}$$

Using upwind method for advection coefficients identified by the superscript u, are given by

$$\begin{aligned} a_1^u &= \max\left[q_{f1}, 0\right] + \max\left[q_{f2}, 0\right] \\ a_2^u &= \max\left[-q_{f1}, 0\right] \\ a_3^u &= \max\left[-q_{f2}, 0\right] \end{aligned} \tag{1.15}$$

The diffusion coefficients, identified with the superscript k, are given by

$$\begin{aligned} a_1^k &= -k_{f1}N_{1x}\Delta\vec{y}_{f1} + k_{f1}N_{1y}\Delta\vec{x}_{f1} - k_{f2}N_{1x}\Delta\vec{y}_{f2} + k_{f2}N_{1y}\Delta\vec{x}_{f2} \\ a_2^k &= -k_{f1}N_{2x}\Delta\vec{y}_{f1} + k_{f1}N_{2y}\Delta\vec{x}_{f1} - k_{f2}N_{2x}\Delta\vec{y}_{f2} + k_{f2}N_{2y}\Delta\vec{x}_{f2}\,. \\ a_2^k &= -k_{f1}N_{3x}\Delta\vec{y}_{f1} + k_{f1}N_{3y}\Delta\vec{x}_{f1} - k_{f2}N_{3x}\Delta\vec{y}_{f2} + k_{f2}N_{3y}\Delta\vec{x}_{f2} \end{aligned} \tag{1.16}$$

In Eq. (1.15), the volume flow across faces 1 and 2 in the direction of the outward normal is

$$\begin{aligned} q_{f1} &= v\cdot nA|_{f1} = v_x^{f1}\Delta\vec{y}_{f1} - v_y^{f1}\Delta\vec{y}_{f1} \\ q_{f2} &= v\cdot nA|_{f2} = v_x^{f2}\Delta\vec{y}_{f2} - v_y^{f2}\Delta\vec{y}_{f2} \end{aligned}. \tag{1.17}$$

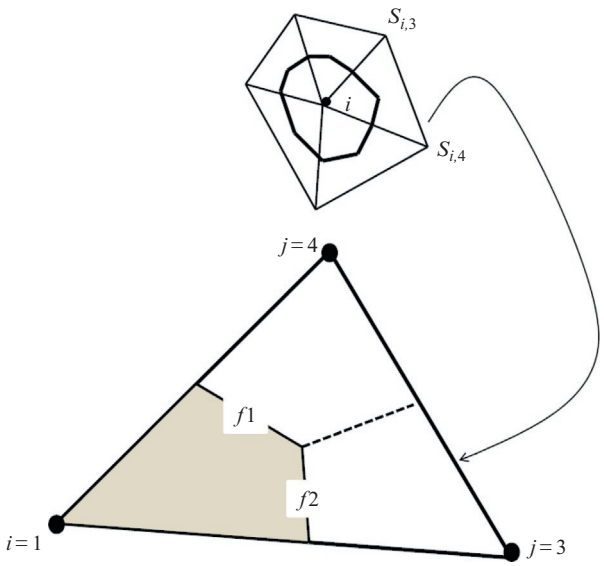

FIGURE 1.4

A sample triangular element and its corresponding control volume.

The value of the diffusivity at the midpoint of face 1 can be obtained as

$$k_{f1} = [N_1k_1 + N_2k_2 + N_3k_3]_{f1} = \frac{5}{12}k_1 + \frac{5}{12}k_2 + \frac{2}{12}k_3 \tag{1.18}$$

and at the midpoint of face 2 as

$$k_{f2} = [N_1k_1 + N_2k_2 + N_3k_3]_{f2} = \frac{5}{12}k_1 + \frac{2}{12}k_2 + \frac{5}{12}k_3. \tag{1.19}$$

The velocity component at the midpoint of face 1 is:

$$\begin{aligned} v_x^{f1} &= \frac{5}{12}v_{x_1} + \frac{5}{12}v_{x_2} + \frac{2}{12}v_{x_3} \\ v_y^{f1} &= \frac{5}{12}v_{y_1} + \frac{5}{12}v_{y_2} + \frac{2}{12}v_{y_3} \end{aligned}. \tag{1.20}$$

On face 2 the velocity component is:

$$\begin{aligned} v_x^{f2} &= \frac{5}{12}v_{x_1} + \frac{2}{12}v_{x_2} + \frac{5}{12}v_{x_3} \\ v_y^{f2} &= \frac{5}{12}v_{y_1} + \frac{2}{12}v_{y_2} + \frac{5}{12}v_{y_3} \end{aligned}. \tag{1.21}$$

These values can be used to update the ith support coefficients using the following equation:

$$\begin{aligned} a_i &= a_i + a_1^k \\ a_{i,3} &= a_{i,3} + a_2^k \\ a_{i,4} &= a_{i,4} + a_3^k \end{aligned}. \tag{1.22}$$

In Eq. (1.16), moving counterclockwise around node i, the signed distances are:

$$\begin{aligned} \Delta\vec{x}_{f1} &= \frac{x_3}{3} - \frac{x_2}{6} - \frac{x_1}{6}, \quad \Delta\vec{x}_{f2} = -\frac{x_2}{3} + \frac{x_3}{6} + \frac{x_1}{6} \\ \Delta\vec{y}_{f1} &= \frac{y_3}{3} - \frac{y_2}{6} - \frac{y_1}{6}, \quad \Delta\vec{y}_{f2} = -\frac{y_2}{3} + \frac{y_3}{6} + \frac{y_1}{6} \end{aligned}, \tag{1.23}$$

the derivatives of the shape functions are:

$$\begin{aligned} N_{1x} &= \frac{\partial N_1}{\partial x} = \frac{(y_2 - y_3)}{2V^{\text{ele}}}, \quad N_{1y} = \frac{\partial N_1}{\partial y} = \frac{(x_3 - x_2)}{2V^{\text{ele}}} \\ N_{2x} &= \frac{\partial N_2}{\partial x} = \frac{(y_3 - y_1)}{2V^{\text{ele}}}, \quad N_{2y} = \frac{\partial N_1}{\partial y} = \frac{(x_1 - x_3)}{2V^{\text{ele}}}, \\ N_{3x} &= \frac{\partial N_2}{\partial x} = \frac{(y_1 - y_2)}{2V^{\text{ele}}}, \quad N_{3y} = \frac{\partial N_3}{\partial y} = \frac{(x_2 - x_1)}{2V^{\text{ele}}} \end{aligned} \tag{1.24}$$

and the volume of the element is

$$V^{\text{ele}} = \frac{(x_2 y_3 - x_3 y_2) + x_1(y_2 - y_3) + y_1(x_3 - x_2)}{2}. \tag{1.25}$$

The obtained algebraic equations from the discretization procedure using CVFEM are solved using the Gauss-Seidel method.

1.5.2 IMPLEMENTATION OF SOURCE TERMS AND BOUNDARY CONDITIONS

The boundary conditions for the present problem can be enforced using B_{B_i} and B_{C_i} as follows [14–16]:

$$\text{Insulated boundary:} \quad B_{B_i} = 0 \quad \text{and} \quad B_{C_i} = 0 \tag{1.26}$$

$$\text{Fixed value boundary:} \quad B_{B_i} = \phi_{\text{value}} \times 10^{16} \quad \text{and} \quad B_{C_i} = 10^{16} \tag{1.27}$$

$$\text{Fixed flux boundary:} \quad B_{B_i} = A_k \times q'' \quad \text{and} \quad B_{C_i} = 0 \tag{1.28}$$

where ϕ_{value} is the prescribed value on the boundary and A_k is the length of the control volume surface on the boundary segment.

To provide a general treatment for boundary conditions, some preliminary calculation of the boundary face areas associated with each node j in a given boundary segment is required. Figure 1.5 shows a schematic of the kth ($k = 3$) boundary, indicating the data structure. Assuming unit depth, the face area associated with any node j of the boundary segment highlighted in Fig. 1.5 is given by

$$A_{k,j} = \begin{cases} \text{Upper}_1 \\ \text{Upper}_j + \text{Lower}_j, \quad 2 \le j \le n_{B,k} - 1 \\ \text{Lower}_{n_{B,k}} \end{cases} \tag{1.29}$$

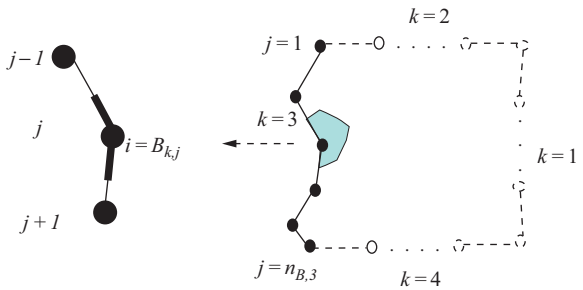

FIGURE 1.5

A domain boundary segment with three sequential points detailed [11].

where

$$\begin{aligned}\text{Upper}_j &= \frac{1}{2}\sqrt{\left(x_j - x_{j+1}\right)^2 + \left(y_j - y_{j+1}\right)^2} \\ \text{Lower}_j &= \frac{1}{2}\sqrt{\left(x_j - x_{j-1}\right)^2 + \left(y_j - y_{j-1}\right)^2}\end{aligned} \tag{1.30}$$

The first and last lines on the right-hand side of Eq. (1.29) account for the first and last node on the boundary segment, respectively. This treatment assumes that there are at least two boundary segments, i.e., at least two contiguous regions of the domain boundary where different boundary conditions are applied. In cases where only one boundary condition is applied (e.g., a constant value over the whole boundary) the condition of a two-segment boundary can be artificially imposed. The volume source terms can be applied to Eq. (1.13) as:

$$\sum_{j=1}^{\text{elements}} \int_{V_j} Q \mathrm{d}V \approx Q_i V_i \tag{1.31}$$

or, after linearizing the source term

$$Q_i V_i = -Q_{C_i}\phi_i + Q_{B_i} \tag{1.32}$$

1.5.3 UNSTEADY ADVECTION-DIFFUSION WITH SOURCE TERMS

The net flow rate of quantity into the control volume around node i can be approximated as

$$Net_i = \int_{V_i} Q \mathrm{d}V + \sum_{j=1}^{n_i} \int_{A^j} \kappa \nabla\phi \cdot n \mathrm{d}A - \int_{A^j} (v \cdot n)\phi \mathrm{d}A \approx -[a_i + Q_{C_i} + B_{C_i}]\phi_i + \sum_{j=1}^{n_i} a_{i,j}\phi_{S_{i,j}} + Q_{B_i} + B_{B_i}. \tag{1.33}$$

In a steady-state problem this flow rate is identically zero. In a transient problem, however, it results in a change in storage of the quantity in the control volume, i.e.,

$$\frac{\mathrm{d}}{\mathrm{d}t}\int_{V_i}\phi\,\mathrm{d}V = \mathrm{Net}_i. \tag{1.34}$$

Using nodal lumping for the volume integration and finite difference in time, this equation can be used to evaluate the nodal field values at time $t+\Delta t$ in terms of the nodal field values at time t,

$$V_i\phi_i^{\mathrm{new}} = V_i\phi_i + \Delta t\left[(1-\theta)\mathrm{Net}_i + \theta\mathrm{Net}_i^{\mathrm{new}}\right], \tag{1.35}$$

where Δt is a time step and the superscript "new" indicates evaluation at time $t+\Delta t$. The parameter $0 \le \theta \le 1$ is a user-defined weighting factor used to approximate the net flow into control volume i during the time interval $[t, t+\Delta t]$ in terms of the net flows at the beginning and end of the time step. Neglecting for now contributions from the boundaries and sources, the resulting discrete equations for three choices of θ are:

Fully implicit $\theta = 1$:

$$V_i\phi_i^{\mathrm{new}} = V_i\phi_i + \Delta t\left(\sum_{j=1}^{n_i} a_{i,j}\phi_{S_{i,j}}^{\mathrm{new}} - a_i\phi_i^{\mathrm{new}}\right) \tag{1.36}$$

The advantage of this choice is that it is unconditionally stable, i.e., for any choice of time step errors (induced or inherent) do not grow. The downside is that a system of equations needs to be solved to obtain the field values at the new time step $\phi_i^{\mathrm{new}}\,(i=1,\ldots,n)$.

Crank-Nicolson $\theta = 0.5$:

$$V_i\phi_i^{\mathrm{new}} = V_i\phi_i + \frac{\Delta t}{2}\left(\sum_{j=1}^{n_i} a_{i,j}\phi_{S_{i,j}}^{\mathrm{new}} - a_i\phi_i^{\mathrm{new}}\right) + \frac{\Delta t}{2}\left(\sum_{j=1}^{n_i} a_{i,j}\phi_{S_{i,j}} - a_i\phi_i\right) \tag{1.37}$$

This unconditionally stable scheme also requires a system solution. Unlike the first-order-in-time, fully implicit method, however, the Crank-Nicolson is second-order-in-time (i.e., time errors scale with Δt^2)

Fully explicit $\theta = 0$:

$$V_i\phi_i^{\mathrm{new}} = V_i\phi_i + \Delta t\left(\sum_{j=1}^{n_i} a_{i,j}\phi_{S_{i,j}} - a_i\phi_i\right) \tag{1.38}$$

This choice can be used to directly update the new time values from the current time values without solving a system of equations. This, however, comes at the price of a restriction on the time step size to ensure stability. The solution of Eq. (1.38) is likely to become unstable (error will increase as the solution advances) if the net coefficient for ϕ_i becomes negative. This requires that the time step is chosen such that

$$\Delta t < \min\left(\frac{V_i}{a_i}\right), \quad (i=1,\ldots,n) \tag{1.39}$$

If a fine grid is used this value could be prohibitively small, i.e., the advance of time could be too slow to reach a practical value using reasonable computational

resources. In many cases, however, the drawback of using a small time step is offset by the ability to solve Eq. (1.29) without iteration. Driven by its simplicity and flexibility of modeling complex nonlinear terms, the explicit time integration approach is the preferred choice in this work. When sources and boundary condition treatments are added, the explicit scheme Eq. (1.29) can be written as

$$(V_i + B_{C_i})\phi_i^{\text{new}} = V_i\phi_i + \Delta t\left(\sum_{j=1}^{n_i} a_{i,j}\phi_{S_{i,j}} - a_i\phi_i + Q_{B_i} - Q_{C_i}\phi_i\right) + B_{B_i} \tag{1.40}$$

The addition of the source term in Eq. (1.40) could require a further reduction in the time step to retain positive coefficients and stability, i.e.,

$$\Delta t < \min\left(\frac{V_i}{a_i + Q_{C_i}}\right), \quad (i = 1, \ldots, n) \tag{1.41}$$

REFERENCES

[1] B.R. Baliga, S.V. Patankar, A new finite element formulation for convection diffusion problems, Numer. Heat Transfer 3 (1980) 393–409.

[2] B.R. Baliga, S.V. Patankar, A control volume finite-element method for two dimensional fluid flow and heat transfer, Numer. Heat Transfer 6 (1983) 245–261.

[3] M.J. Raw, G.E. Schneider, A skewed, positive influence coefficient up-winding procedure for control volume based finite element convection-diffusion computation, Numer. Heat Transfer 9 (1986) 1–26.

[4] M.J. Raw, G.E. Schneider, V. Hassani, A nine-noded quadratic control volume based finite element for heat conduction, J. Spacecraft 22 (1985) 523–529.

[5] J. Banaszek, Comparison of control volume and Galerkin finite element methods for diffusion type problems, Numer. Heat Transfer 16 (1989) 59–78.

[6] J.B. Campos Silva, E.D.R. Vieira, L.F.M. Moura, Control volume finite element and flow visualization methods applied for unsteady viscous flow past a circular cylinder, in: Proc. V Congresso de Engenhari a Mecanica do Norte-Nordeste, Fortaleza, CE, Brazil, vol. II, 1998, pp. 80–87.

[7] J.B. Campos Silva, L.F.M. Moura, Numerical simulation of fluid flow by the control volume finite element method, in: Proceedings (in CD-ROM) of the XIV Brazilian Congress of Mechanical Engineering (COBEM97), Bauru, SP, Brazil, 1997, pp. 1–8, (Paper Code 041).

[8] J.B. Campos Silva, Numerical Simulation of Fluid Flow by the Finite Element Method Based on Control Volumes, Ph.D. ThesisState University of Campinas, Campinas, SP, Brazil, 1998 (in Portuguese).

[9] H.J. Saabas, B.R. Baliga, Co-located equal order control volume finite element method for multidimensional incompressible fluid flow—part I: formulation, Numer. Heat Transfer 26 (1994) 381–407.

[10] H.J. Saabas, B.R. Baliga, Co-located equal order control volume finite element method for multidimensional incompressible fluid flow—part II: verification, Numer. Heat Transfer B 26 (1994) 409–424.

[11] V.R. Voller, Basic Control Volume Finite Element Methods for Fluids and Solids, World Scientific Publishing Co. Pte. Ltd. 5, Tohccxxvc, 2009.
[12] M. Sheikholeslami, M. Gorji-Bandpy, I. Pop, S. Soleimani, Numerical study of natural convection between a circular enclosure and a sinusoidal cylinder using control volume based finite element method, Int. J. Therm. Sci. 72 (2013) 147–158.
[13] D.W. Pepper, Meshless methods, in: W.J. Minkowycz, E.M. Sparrow, J.Y. Murthu (Eds.), Handbook of Numerical Heat Transfer, Wiley, Hoboken, 2006.
[14] M. Sheikholeslami, R. Ellahi, M. Hassan, S. Soleimani, A study of natural convection heat transfer in a nanofluid filled enclosure with elliptic inner cylinder, Int. J. Numer. Methods for Heat & Fluid Flow 24 (8) (2014) 1906–1927.
[15] M. Sheikholeslami Kandelousi, Effect of spatially variable magnetic field on ferrofluid flow and heat transfer considering constant heat flux boundary condition, Eur. Phys. J. Plus (2014) 129–248.
[16] M. Sheikholeslami, D.D. Ganji, M.M. Rashidi, Ferrofluid flow and heat transfer in a semi annulus enclosure in the presence of magnetic source considering thermal radiation, J. Taiwan Inst. Chem. Eng. (2014), in press. http://dx.doi.org/10.1016/j.jtice.2014.09.026.